The Calculation of Temperature and Thermal Stress Distributions in the Planar Solid Oxide Fuel Cell

Kiyoshi KANAMURA,* Shoji YOSHIOKA, and Zen-ichiro TAKEHARA
Department of Industrial Chemistry, Faculty of Engineering, Kyoto University, Yoshida-honmachi, Sakyo-ku, Kyoto 606
(Received August 28, 1991)

The temperature and thermal stress distributions in a planar solid oxide fuel cell (SOFC) were calculated using a finite element method in order to determine guidelines for the selection of cell materials. The calculations indicate that the thermal stress is generated in a planar SOFC composed of yttria stabilized zirconia (YSZ) electrolyte, a $LaMnO_3$ cathode, and a Ni-YSZ cermet anode. The largest stress is generated in the region of the cathode material. According to the calculations, if the linear expansion of the cathode material is 1.0×10^{-6} (the linear expansion of porous $LaMnO_3$ is 2.0×10^{-5}), the thermal stress in the SOFC will be relieved.

The solid oxide fuel cell (SOFC) is one of the most promising types of fuel cells, because of its high energy utilization. In SOFC, an ionically-conductive oxide, such as yttria stabilized zirconia, is used as the electrolyte. Yttria stabilized zirconia (YSZ) has an excellent conductivity around 1273 K, and consequently, SOFC is operated at high temperature. The electrodes, electrolyte, and other materials all consist of oxides. Recently, SOFC composed of thin films of these oxides have been prepared by chemical or physical vapor deposition methods.[1-3] Such a SOFC has a low ohmic resistance, and a correspondingly low energy loss. The mechanical stability of SOFC depends on the cell materials used: Differing thermal expansions amongst the different cell materials can generate significant mechanical stresses. Estimation of the thermal stress distribution in SOFC may be helpful in determining the compatibility and suitability of materials for the construction of SOFC. In this study, the temperature and thermal stress distributions in the small planar solid oxide fuel cell were calculated in order to demonstrate the importance of the heat management in solid oxide fuel cells.

Model of Planar SOFC and Operating Conditions

Recently, many kinds of materials for SOFC have been developed to improve the cell performance. The physical properties of these materials are different. In this study, it was assumed that the model SOFC was of the most common type, consisting of a porous $LaMnO_3$ cathode, a porous Ni-YSZ cermet anode, YSZ electrolyte, and a porous YSZ support. Schematic illustrations of the model SOFC and its size are summarized in Fig. 1. The cell is supported at the two ends, as shown in Fig. 1. The thermal expansion of the support is assumed to be much less than those of the materials consisting of SOFC (nearly equal 0). In other words, the cell is fixed at two side walls. In this study, the temperature and thermal stress distributions in the small planar SOFC were calculated. Hydrogen gas flows through the anode chamber and air flows through the cathode chamber. The typical operating parameters used in the calculation of the temperature and the thermal stress distributions for the planar SOFC are listed in Table 1. The electrochemical parameters have

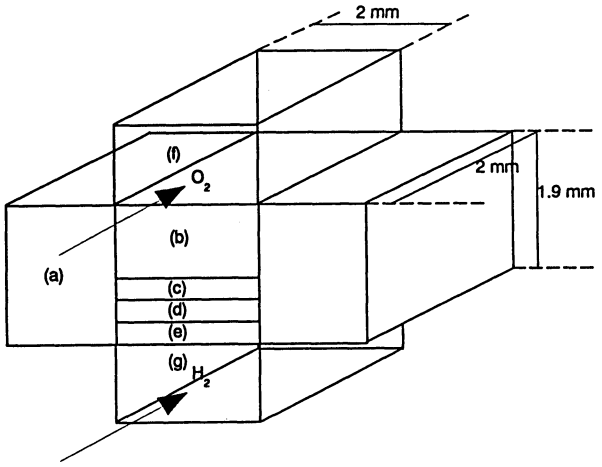

Fig. 1. Schematic illustration of the small planar solid oxide fuel cell, (a): support, (b): porous substrate, (c): porous cathode, (d): YSZ electrolyte, (e): porous anode, (f): oxygen chamber, (g): fuel chamber.

Table 1. Operating Conditions for the Calculation of the Temperature and Thermal Stress Distributions in the Small Planar SOFC

Conditions	Values
Temperature of gas	1273 K
Partial pressure of hydrogen	0.95×10^5 Pa
Partial pressure of oxygen	0.21×10^5 Pa
Apparent current density	500 mA cm^{-2}
Roughness factor of anode	100

been investigated by many researchers.[4-11] Some physical properties depend on the temperature. In this calculation, it is assumed that these parameters are independent of the temperature. The exchange currents for anodic and cathodic reactions depend on the kinds of electrodes. In our model, the overpotential of cathode reaction is assumed to be negligibly small comparing with other resistances.[12]

Temperature Distribution in Planar SOFC

The model used in this study corresponds to one of the part of the practical planar SOFC. The partial pressures of hydrogen and oxygen are assumed to be constant at 0.95×10^5 Pa and 0.21×10^5 Pa, respectively. The overpotentials and the entropy changes of the electrode reactions and the ohmic resistance of the YSZ were taken into account when calculating the heat generation or absorption. The entropy change of oxygen electrode reaction was estimated to be 81.6 $J\,mol^{-1}\,K^{-1}$ per two electrons from Seebeck coefficient measurement.[13] The entropy change of hydrogen electrode reaction was calculated from the total entropy change, which was estimated from the thermodynamic data, and the entropy change of oxygen electrode reaction. The entropy changes of hydrogen and oxygen under various partial pressures were calculated, according to the reference.[14] In the calculation, the term of the entropy change is very important. Because, in the electrochemical system operating at high temperature, the entropy change is the largest heat source. The following equations were assumed for the heat generation and the overpotential.

For the cathode:

$$\frac{dQ}{dt} = IT\Delta S_c + I\eta_c, \tag{1}$$

$$\eta_c = 0, \tag{2}$$

where η_c and ΔS_c are the overpotential and the entropy change of the cathode reaction, I is the current, Q is the amount of heat produced, and t is the time.

For the anode:

$$\frac{dQ}{dt} = IT\Delta S_a + I\eta_a, \tag{3}$$

$$\eta_a = K\ln(I/I_o), \tag{4}$$

where, I_o is the exchange current for hydrogen oxidation, η_a and ΔS_a are the overpotential and the entropy change of the anode reaction, respectively. The heat generation due to the ohmic resistance of the YSZ was estimated as

$$\frac{dQ}{dt} = I^2R, \tag{5}$$

where $R=(L/S)(1/\sigma)$, and σ is the conductivity of YSZ, L is the thickness of the YSZ electrolyte, and S is the surface area of the YSZ electrolyte. These heat generation factors are summarized in Fig. 2. The parameters are obtained from the references and are summarized in Table 2.[15,16] The amount of heat generated in each part of SOFC was listed in Table 3. The thermal parameters of the materials composing the planar SOFC used in this calculation were estimated from the

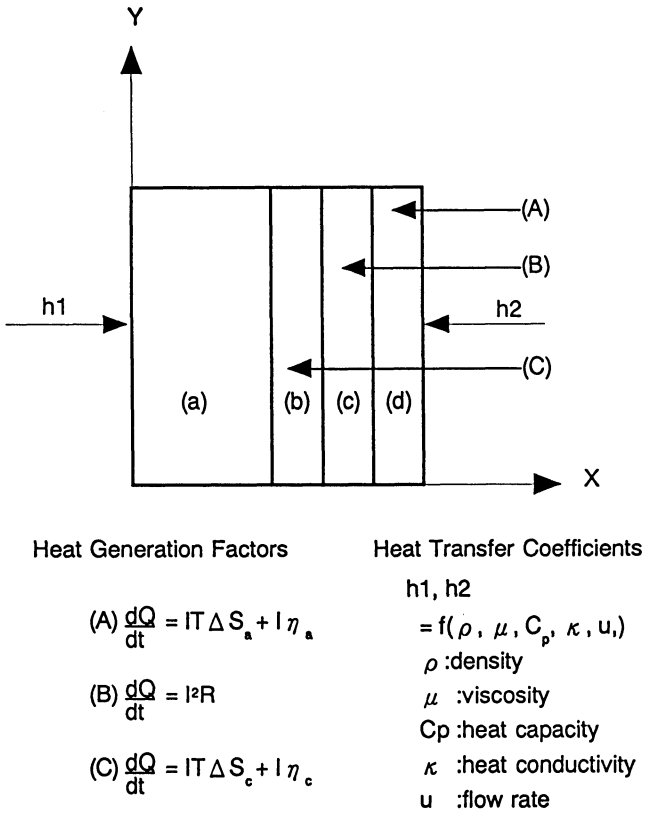

Fig. 2. Heat generation factors and heat transfer coefficients for the calculation of the temperature distribution in the small planar solid oxide fuel cell, (a): porous substrate, (b): porous cathode, (c): YSZ electrolyte, (d): porous anode.

Table 2. Electrochemical Parameters for the Anode of the Small Planar SOFC

Electrochemical parameters	Values
I_o[a]	0.98 mA cm^{-2}
K[b]	0.0609 V
σ[c]	0.1 S cm^{-1}

a) From Ref. 4. b) $K=RT/4\alpha F$, α: transfer coefficient, R: gas constant, F: Faraday constant, from Ref. 4. c) $R=(1/\sigma)(L/S)$, L: thickness of YSZ of element, surface area of YSZ of element, from Ref. 12.

Table 3. Amount of Heat Generated at Each Part of the Small Planar SOFC

Part		Amount of heat/J s^{-1}
Cathode		0.00539
Anode	Total	−0.00186
	(Entropy term	−0.00284)
	(Overpotential	0.00098)
Electrolyte		0.00048

Table 4. Heat Conductivities of the Materials in the Small Planar SOFC

Material	Heat conductivity/J s^{-1} cm^{-1} K^{-1}
YSZ	0.027
$LaMnO_3$	0.06
Ni	0.42

extrapolation of the values reported in the reference,[15,16] as shown in Table 4. Moreover, the porosities of the cathode, the anode, and the electrolyte were considered in the estimation of the thermal conductivities, according to the following equation. The porosity of these materials were assumed to be 30%. The porous cathode, the porous anode, and the porous substrate were treated as the mixed phase of the gas and their materials.

$$k_m = k_c \frac{1+2v_d(1-k_c/k_d)/(2k_c/k_d+1)}{1-2v_d(1-k_c/k_d)/(2k_c/k_d+1)}, \quad (6)$$

where, k_m is the heat conductivity of the mixed phase, k_c is the heat conductivity of the cell materials, k_d is that of the gas, and v_d is the volume ratio between the cell materials and the gas. The heat conductivity of Ni cermet (porosity: 40%) was also estimated from this equation. At the interfaces between the anode and hydrogen gas and the porous YSZ support and oxygen gas, the heat transfer coefficients were assumed, as shown in Fig. 2. The heat transfer coefficients were estimated to be 10^{-3} J s^{-1} cm^{-2} K^{-1}. These coefficients depend on the flow rate of gas and the shape of the chamber. In this study, the laminar flow was assumed and its flow rate was assumed to be 20 cm s^{-1}.

Figure 3 shows the resulting temperature distribution in the planar SOFC calculated by using a finite element method.[17] The temperature of the gas was assumed to be constant at 1273 K. The initial temperature of all parts of the small planar SOFC was assumed to be 300 K. The largest temperature gradient was observed at the interface between the cathode and the porous YSZ support. The maximum temperature was observed in the cathode region. The amount of heat generated from the entropy change of the cathode reaction is significantly large and is comparable with the sum of the heat generated from the overpotential of the cathode and the ohmic resistance of the YSZ electrolyte under the operating conditions assumed in this study. In this model, the cathode is the largest heat source, as shown in Table 3. The overpotentials of cathode and anode and the ohmic resistance of YSZ will be improved. However the heat produced by the entropy changes of cathode and anode can not be improved, because of the thermodynamic limitation. Therefore, the term of the entropy will become more important in the calculation of the temperature and thermal stress distributions.

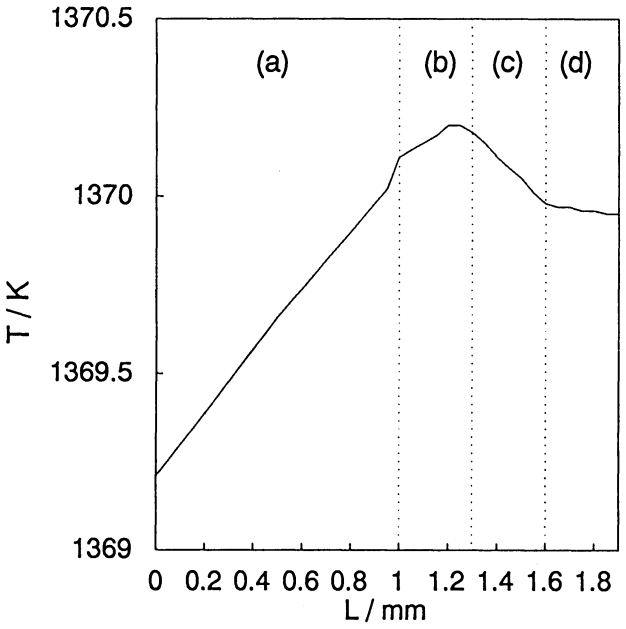

Fig. 3. The temperature distribution in the small planar solid oxide fuel cell, (a): porous substrate, (b): porous cathode, (c): YSZ electrolyte, (d): porous anode.

Thermal Stress Distribution

The temperature difference between the materials in SOFC results in the generation of the stress in all materials of the SOFC and at the interfaces between the materials. Such a stress is the cause of the deconstruction of the SOFC. In this study, the calculation of the thermal stress in the small planar SOFC was demonstrated using the same model used in the calculation of the temperature distribution. The thermal stress distribution was calculated using a finite element method from the temperature distribution obtained in the previous section.[17] The values of the mechanical properties of the cell materials that were used in the calculation are summarized in Table 5, which were obtained from the references.[15] The modulus of elasticity for the

Table 5. Coefficients of Linear Expansion, Modulus of Elasticity, and Poisson's Ratio of the Cell Materials

Materials	Coefficient of linear expansion	Modulus of elasticity	Poisson's ratio
YSZ	3.8×10^{-6}	1.55×10^{8}	0.25
Porous YSZ substrate	3.3×10^{-6}	7.91×10^{7}	0.25
Porous cathode	2.0×10^{-5}	7.08×10^{8}	0.25
Porous anode	1.7×10^{-5}	3.59×10^{7}	0.4

porous materials was estimated using the empirical equation

$$E = E_0 (1 - 1.9P + 0.9P^2), \quad (7)$$

where P is the porosity. It was assumed to be 30%.

Figure 4 shows the calculated thermal stress distribution in the planar SOFC. σ_{xx} and σ_{yy} are the principal stresses and σ_{xy} is the shearing stress. The principal stress along the x-axis is almost zero in the whole region. The cell expands along x-direction. On the other hand, the principal stress along the y-axis is very large, especially in the region of the cathode. Along y-direction, the cell cannot expand. The thermal expansion of the supports are assumed to be 0. At the interface between the porous YSZ substrate and the cathode, the shearing stress was observed. If the deconstruction of the planar SOFC is caused by the shearing stress, the interface between cathode and the porous substrate materials is the most possible site. The absolute value of the shearing stress in this model might be insignificant for the deconstraction of the cell. However the practical cell is much larger than the model used in this study. The stress increases with increasing size of the cell. Therefore the stress generated in this model is significant. The thermal expansion coefficient of the cathode should be the same with that of the porous substrate.

Figure 5 shows the principal stress along the y-axis, when the coefficient of linear expansion is 1.0×10^{-6}. The principal stress in the cathode is much smaller than that in Fig. 4. The principal stress in other regions also became smaller. Thus, the cathode material is important for the stability of the planar SOFC. Figure 6 shows the effect of the coefficient of linear expansion of the cathode material on the principal stress in the cathode. The principal stress changes with the coefficient of linear expansion, linearly. The deconstruction

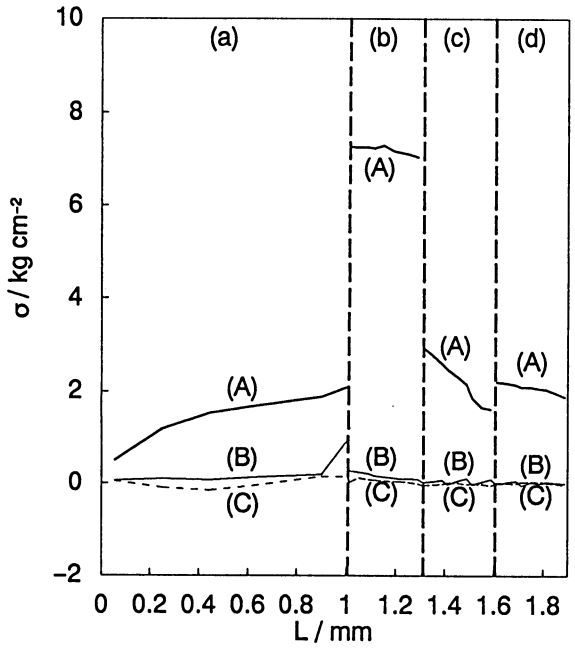

Fig. 4. The thermal stress distribution in solid oxide fuel cell in the small planar solid oxide cell, (A): principal stress along y axis (σ_{yy}), (B): shearing stress (σ_{xy}), (C): principal stress along x axis (σ_{xx}), (a): porous substrate, (b): porous cathode, (c): YSZ electrolyte, (d): porous anode.

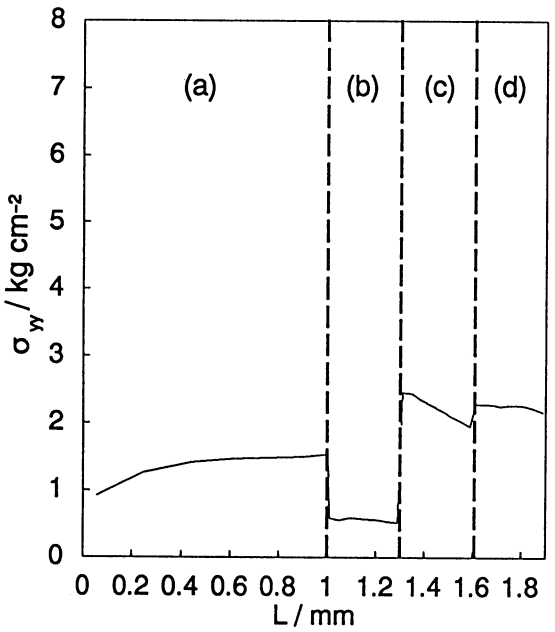

Fig. 5. The principal stress distribution along the y axis when the coefficient of linear expansion of the cathode material is assumed to be 1.0×10^{-6}, (a): porous substrate, (b): porous cathode, (c): YSZ electrolyte, (d): porous anode.

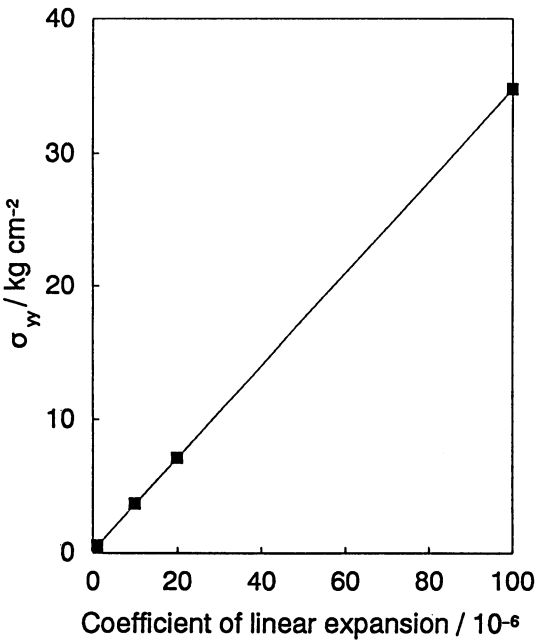

Fig. 6. Dependence of the principal stress along y axis in the cathode region on the coefficient of linear expansion of the cathode material.

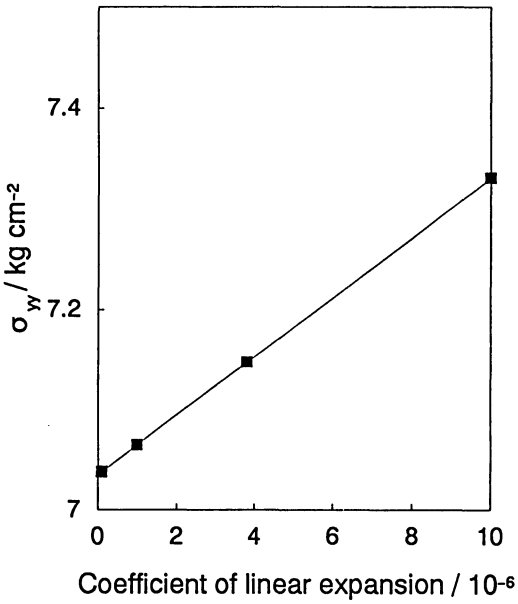

Fig. 7. Dependence of the principal stress along y axis in the cathode region on the coefficient of linear expansion of the substrate material.

of the cell can be prevent by the proper selection of the cathode material. However the cathode must have the good electrochemical characteristics and the thermal stability at 1273 K. Almost the cathode materials are the perovskite or the spinel type transition metal oxides. The coefficient of linear expansion of these oxides would not be changed in the wide range.

Figure 7 shows the effect of the coefficient of the linear expansion of the porous substrate on the principal stress in the cathode region. The principal stress in the cathode region increased with increasing coefficient of the linear expansion of the substrate. The mechanical property of the porous substrate influences the principal stress in the cathode region. The principal stress in the cathode region may be decreased by the suitable selection of the porous substrate. However the effect of the coefficient of the linear expansion of the substrate was much smaller than that of the cathode.

References

1) A. Negishi, K. Nozaki, and T. Ozawa, *Solid State Ionics,* **3/4**, 443 (1981).
2) M. F. Carolan and J. N. Michaels, *Solid State Ionics,* **25**, 207 (1987).
3) A. O. Isenberg, *Solid State Ionics,* **3/4**, 489 (1981).
4) N. J. Maskalick and D. K. Mclain, *J. Electrochem. Soc.,* **135**, 6 (1988).
5) E. J. L. Schouler, M. Kleitz, E. Forest, E. Fernandez, and P. Fabry, *Solid State Ionics,* **3/4**, 531 (1981).
6) J. Sasaki, J. Mizusaki, and Z. Kozuka, *Solid State Ionics,* **3/4**, 495 (1981).
7) G. B. Barbi and C. M. Mari, *Solid State Ionics,* **26**, 243 (1988).
8) J. Mizusaki, K. Amano, S. Yamauchi, and K. Fueki, *Solid State Ionics,* **22**, 313 (1987).
9) J. Mizusaki, K. Amano, S. Yamauchi, and K. Fueki, *Solid State Ionics,* **22**, 323 (1987).
10) H. Nafe, *Solid State Ionics,* **13**, 255 (1984).
11) E. J. L. Schouler, N. Mesbahi, and G. Vitter, *Solid State Ionics,* **9/10**, 989 (1983).
12) N. J. Maskalick, "Proceedings of The First International Symposium on Solid Oxide Fuel Cell," ed by S. C. Sihghal, Hollywood, Fla. (1989), Vol. 89—11, p. 279.
13) Z. Takehara, K. Kanamura, and S. Yoshioka, *J. Electrochem. Soc.,* **136**, 2506 (1989).
14) K. Kanamura, S. Yoshioka, and Z. Takehara, *J. Electrochem. Soc.,* **138**, 2165 (1991).
15) W. D. Kingery, H. K. Bowen, and D. R. Uhlmann, "Introduction to Ceramics," John Wily & Sons, New York (1976), p. 642.
16) Y. Ohno, S. Nagata, and H. Sato, *Solid State Ionics,* **9 & 10**, 979 (1983).
17) M. Simoseki and H. Fujinuma, "PC-9801 Finite Element Method/Thermal Stress under Non-Steady State Programing," Nikkan Kogyo Shinbunsha, Tokyo (1989).